



King's Research Portal

DOI:

[10.3324/haematol.2018.214767](https://doi.org/10.3324/haematol.2018.214767)

Document Version

Peer reviewed version

[Link to publication record in King's Research Portal](#)

Citation for published version (APA):

Cheung, T. S., Galleu, A., von Bonin, M., Bornhäuser, M., & Dazzi, F. (2019). Apoptotic mesenchymal stromal cells induce prostaglandin E2 in monocytes: Implications for the monitoring of mesenchymal stromal cell activity. *Haematologica*, 104(10), e438-e441. <https://doi.org/10.3324/haematol.2018.214767>

Citing this paper

Please note that where the full-text provided on King's Research Portal is the Author Accepted Manuscript or Post-Print version this may differ from the final Published version. If citing, it is advised that you check and use the publisher's definitive version for pagination, volume/issue, and date of publication details. And where the final published version is provided on the Research Portal, if citing you are again advised to check the publisher's website for any subsequent corrections.

General rights

Copyright and moral rights for the publications made accessible in the Research Portal are retained by the authors and/or other copyright owners and it is a condition of accessing publications that users recognize and abide by the legal requirements associated with these rights.

- Users may download and print one copy of any publication from the Research Portal for the purpose of private study or research.
- You may not further distribute the material or use it for any profit-making activity or commercial gain
- You may freely distribute the URL identifying the publication in the Research Portal

Take down policy

If you believe that this document breaches copyright please contact librarypure@kcl.ac.uk providing details, and we will remove access to the work immediately and investigate your claim.



Journal of The Ferrata Storti Foundation

Apoptotic mesenchymal stromal cells induce prostaglandin E2 in monocytes: implications for the monitoring of mesenchymal stromal cells activity

by Tik Shing Cheung, Antonio Galleu, Malte von Bonin, Martin Bornhäuser, and Francesco Dazzi

Haematologica 2019 [Epub ahead of print]

Citation: Tik Shing Cheung, Antonio Galleu, Malte von Bonin, Martin Bornhäuser, and Francesco Dazzi. Apoptotic mesenchymal stromal cells induce prostaglandin E2 in monocytes: implications for the monitoring of mesenchymal stromal cells activity.

Haematologica. 2019; 104:xxx

doi:10.3324/haematol.2018.214767

Publisher's Disclaimer.

E-publishing ahead of print is increasingly important for the rapid dissemination of science. Haematologica is, therefore, E-publishing PDF files of an early version of manuscripts that have completed a regular peer review and have been accepted for publication. E-publishing of this PDF file has been approved by the authors. After having E-published Ahead of Print, manuscripts will then undergo technical and English editing, typesetting, proof correction and be presented for the authors' final approval; the final version of the manuscript will then appear in print on a regular issue of the journal. All legal disclaimers that apply to the journal also pertain to this production process.

Title

Apoptotic mesenchymal stromal cells induce prostaglandin E₂ in monocytes: implications for the monitoring of mesenchymal stromal cell activity

Tik Shing Cheung¹, Antonio Galleu¹, Malte von Bonin², Martin Bornhäuser²,
Francesco Dazzi^{1*}

¹School of Cancer and Pharmacological Sciences and KHP Cancer Research UK Centre, King's College London, London, United Kingdom. ²University Hospital Carl Gustav Carus, Dresden, Germany.

*Corresponding author. Email address: francesco.dazzi@kcl.ac.uk

Letter to the Editor

The extensive experience with mesenchymal stromal cells (MSCs) in the treatment of inflammatory disorders has provided convincing evidence to support their clinical efficacy in selected cases, especially in steroid-resistant acute graft-versus-host disease (GvHD)^{1,2}. Although MSCs can directly induce immunosuppression through the secretion of soluble factors and contact-mediated mechanisms, it is becoming clearer that the recruitment of recipient immunoregulatory networks is fundamental for delivering their therapeutic effects³. We have recently identified a novel mechanistic pathway by which MSCs mediate immunosuppression in GvHD⁴. Following contact with recipient cytotoxic cells, MSCs undergo *in vivo* apoptosis and are efferocytosed by phagocytes which are then induced to up-regulate indoleamine 2,3-dioxygenase (IDO). Therefore, to accomplish MSC immunosuppression, patients must harbor activated cytotoxic cells and competent phagocytes. Whilst assessing the magnitude of MSC apoptosis induced by recipient cytotoxic cells can provide a biomarker predictive of clinical responses to MSC⁴, there are no tools to monitor the immunological effects of MSC following efferocytosis. In order to identify potential molecules for monitoring MSC immunological effects in patients, we interrogated the molecular and functional profile of human monocytes exposed to apoptotic MSCs (ApoMSCs).

We isolated CD14⁺ monocytes from the peripheral blood of healthy donors (Supplementary Methods) because of their recognized role in engulfing dead MSCs⁵. MSCs were isolated and expanded as previously described⁴, and induced to undergo apoptosis using anti-Fas monoclonal antibody (CH11, Merck). ApoMSCs were characterized by Annexin-V (BD Biosciences) staining and immunoblotting for activated caspase-3 (Cell signaling) (Supplementary Methods & Supplementary Figure S1A-C). CellTrace™Violet (Thermo Fisher Scientific)-labelled (staining concentration: 1 μM) monocytes were cultured with ApoMSCs labelled with 20 ng/mL pH-sensitive fluorescent dye pHrodo™Red⁶ (Thermo Fisher Scientific). Efferocytosis was determined by quantitating pHrodo™Red fluorescence (mean fluorescence intensity, MFI) in monocytes using flow cytometry or CSU-X1 Spinning-Disk Confocal. Confocal data were processed with NIS Elements AR (Nikon) software. After 2 hours, monocytes

rapidly engulfed ApoMSCs but not the non-apoptotic MSCs (Supplementary Figure S2A–B). ApoMSC efferocytosis was enhanced in the presence of lipopolysaccharide (LPS, 100µg/mL, Sigma–Aldrich) to model inflammation⁷ (Figure 1A). When exposure to ApoMSCs was extended to 24 hours, the magnitude of efferocytosis was increased (Figure 1B–C).

Apoptotic cell clearance is generally regarded as immune–silencing, although under particular circumstances, it can elicit immune responses⁸. To examine the immunomodulatory activity of ApoMSC–conditioned monocytes (ApoMSC–Mono), we measured their ability to inhibit CD3/CD28–induced T–cell proliferation. CD3 T cells were isolated from the peripheral blood of healthy donors (Supplementary Methods). Monocytes were cultured with ApoMSCs for 8 hours, and then added to CellTrace™Violet–labelled T cells (10^3 cells/µL) stimulated with CD3/CD28 (Thermo Fisher Scientific) at 1:1 cell–to–bead ratio for 3 days. The proportion of proliferating T–cells was quantitated using flow cytometry. Remarkably, the ApoMSC–conditioned monocytes (ApoMSC–Mono) inhibited 50% of the T–cell proliferation in relative to the monocytes or ApoMSCs alone (Figure 1D). In contrast, ApoMSCs alone did not exhibit any inhibitory effect, suggesting that monocytes are required to inhibit the T–cell proliferation. Besides, it also excludes the possibility that there are any remaining non–apoptotic MSCs producing immunosuppressive effects.

We then characterized the molecular profile of ApoMSC–Mono by evaluating the expression of selected molecules known to effect immunosuppression. CellTrace™Violet–labelled monocytes were cultured with ApoMSCs. After 8 hours, the monocytes were stained with anti–human IDO–PE (eyedio), cyclooxygenase2 (COX2)–PE (AS67) and programmed death–ligand 1 (PD–L1)–PE–Cy7 (29E.2A3) antibody and analyzed using flow cytometry. Notably, IDO, COX2 and PD–L1 were significantly up–regulated in ApoMSC–Mono (Figure 1E–G). Examining the secreted soluble factors in culture supernatant, ELISA methods were used (all Thermo Fisher Scientific). We found the secretion of PGE₂ and interleukin–10 (IL–10) was markedly increased, but tumor necrosis factor–α (TNF–α) was reduced compared to monocytes or ApoMSCs alone (Figure H–J). Overall the data suggest that monocytes exhibited a functional and molecular immunosuppressive phenotype following efferocytosis of ApoMSCs.

To confirm the association between efferocytosis and the production of these immunosuppressive molecules, ApoMSCs were labelled with CellTrace™FarRed (APC, Thermo Fisher Scientific) (Figure 1K). The increased expression of COX2, IDO and PD-L1 was selectively detected in the monocytes engulfing ApoMSCs (APC+) (Figure 1K-L).

Intriguingly, previous studies have indicated the ability of PGE₂ to induce IDO, PD-L1 and IL-10⁹⁻¹¹. Therefore, we investigated the dependence of these molecules on COX2/PGE₂ activity. During the monocyte-conditioning, the selective COX2 inhibitor NS-398 (100 μM, Cayman) was added to inactivate COX2 in monocytes. The COX2 inhibition of monocytes was sufficient to prevent the induction of IDO, PD-L1 and IL-10, without interfering with efferocytosis (Figure 2A-E). Importantly, it significantly impaired the immunosuppressive activity of ApoMSC-Mono on *in vitro* T-cell proliferation (Figure 2F). Collectively, these findings reveal the ultimate role of efferocytosis-induced COX2/PGE₂ in delivering immunosuppression and its master role in regulating IDO, PD-L1 and IL-10 induced by efferocytosis. According to previous studies, PGE₂ may enhance the expression of IDO or IL10 through the induction of cyclic adenosine monophosphate and protein kinase A activation^{9,11}.

Since COX2/PGE₂ is the key effector of ApoMSC-induced immunosuppressive monocytes, we asked whether PGE₂ levels could reflect the MSC immunological activity in GvHD patients receiving MSC treatment. This choice presents a major advantage compared to monitoring IDO activity. Although we previously identified IDO as the ultimate effector of ApoMSC in GvHD, the current method of determining IDO activity¹² remains to be optimized. Soluble factors such as PGE₂ serve as a simpler and more cost-effective approach for monitoring MSC immunological effects.

Between July 2016 and August 2017, 8 severe steroid-resistant GvHD patients were treated with MSCs at the University Hospital Carl Gustav Carus (TU Dresden, Germany). MSCs were generated from the bone marrow of multiple third-party donors and expanded under good-manufacturing-practice conditions in Dresden Stem Cell Laboratory¹³. The treatment was made

according to Regulation (European Commission) no. 1394/2007. The patient characteristics are summarized in Table 1. The diagnosis of GvHD was made according to standard criteria¹⁴. Clinical responses to MSCs, defined by at least 1 stage reduction in any GvHD organ after infusion, were assessed 1 week after the infusion^{1,13}. Donors and patients provided informed consent (Technische Universität Dresden, EK206082008).

The average MSC dose was $1.68 \pm 0.62 \times 10^6/\text{kg}$ (Mean \pm SD), ranging from 1.02 to $2.28 \times 10^6/\text{kg}$. 4 patients achieved a partial response. One of the responder patients received two independent MSC infusions and assessed twice accordingly. 4 patients were non-responders. Serum samples were collected from patients 1 day before MSC infusion and then between 1 and 4 days (median 4 days) after the infusion and examined for PGE₂ levels (Figure 2G, Supplementary Figure S3A–B). In order to compare the results across patients, we calculated the change in PGE₂ levels before and after MSC infusion using the formula $[\text{PGE}_2^{\text{after infusion}} - \text{PGE}_2^{\text{before infusion}}]/\text{PGE}_2^{\text{before infusion}} \times 100\%$. As a result, the percentage of PGE₂ increment was significantly higher in clinical responders compared to non-responders in which PGE₂ levels remained unchanged (Figure 2G). We are aware that the number of patients assessed is small and larger prospective studies are needed to validate our findings. Furthermore, it would be interesting to assess whether the phagocytes in responders and non-responders exhibit any functional difference in efferocytosis.

Overall, this study further strengthens the role of *in vivo* MSC apoptosis in delivering immunosuppression^{4,15}. By showing that efferocytosis of ApoMSCs results in PGE₂-dependent immunosuppression, our study is a step forward towards our understanding of the immunomodulatory role of MSC apoptosis. Therefore, we suggest that PGE₂ monitoring could estimate the immunological activity of MSC therapy in GvHD patients.

Acknowledgements

- TSC is recipient of the Hong Kong Scholarships by The King's College London Hong Kong Foundation Ltd and the Chinese Student Awards by the Great Britain–China Educational Trust
- This work was funded by the Bloodwise Specialist Programme 14019
- AG is recipient of the Bloodwise Clinical Training Fellowship 15029

Authorship Contributions

FD and AG conceptualized the study; TSC and AG developed the methodology; TSC conducted the investigation; MvB and MB treated and investigated the patients; TSG and FD wrote the manuscript. AG, MvB and MB reviewed and edited the manuscript; FD acquired the funding and supervised the study

Disclosure of Conflicts of Interest

The authors declare that they have no competing interests

References

1. Galleu A, Milojkovic D, Deplano S, et al. Mesenchymal stromal cells for acute graft-versus-host disease: response at 1 week predicts probability of survival. *Br J Haematol*. 2019 Jan 13. [Epub ahead of print].
2. Le Blanc K, Frassoni F, Ball L, et al. Mesenchymal stem cells for treatment of steroid-resistant, severe, acute graft-versus-host disease: a phase II study. *Lancet*. 2008;371(9624):1579-1586.
3. Cheung TS, Dazzi F. Mesenchymal-myeloid interaction in the regulation of immunity. *Semin Immunol*. 2018;35:59-68.
4. Galleu A, Riffo-Vasquez Y, Trento C, et al. Apoptosis in mesenchymal stromal cells induces in vivo recipient-mediated immunomodulation. *Sci Transl Med*. 2017;9(416).
5. de Witte SFH, Luk F, Sierra Parraga JM, et al. Immunomodulation By Therapeutic Mesenchymal Stromal Cells (MSC) Is Triggered Through Phagocytosis of MSC By Monocytic Cells. *Stem Cells*. 2018;36(4):602-615.
6. Miksa M, Komura H, Wu R, Shah KG, Wang P. A novel method to determine the engulfment of apoptotic cells by macrophages using pHrodo succinimidyl ester. *J Immunol Methods*. 2009;342(1-2):71-77.
7. Raetz CRH, Whitfield C. Lipopolysaccharide Endotoxins. *Annu Rev Biochem*. 2002;71(1):635-700.
8. Yatim N, Cullen S, Albert ML. Dying cells actively regulate adaptive immune responses. *Nat Rev Immunol*. 2017;17(4):262-275.
9. Braun D, Longman RS, Albert ML. A two-step induction of indoleamine 2,3 dioxygenase (IDO) activity during dendritic-cell maturation. *Blood*. 2005;106(7):2375-2381.
10. Prima V, Kaliberova LN, Kaliberov S, Curiel DT, Kusmartsev S. COX2/mPGES1/PGE2 pathway regulates PD-L1 expression in tumor-associated macrophages and myeloid-derived suppressor cells. *Proc Natl Acad Sci U S A*. 2017;114(5):1117-1122.
11. MacKenzie KF, Clark K, Naqvi S, et al. PGE2 Induces Macrophage IL-10 Production and a Regulatory-like Phenotype via a Protein Kinase A-SIK-CRTC3 Pathway. *J Immunol*. 2013;190(2):565-577.
12. Du T ting, Cui T, Qiu H mei, Wang N ru, Huang D, Jiang X hui. Simultaneous determination of tryptophan, kynurenine, kynurenic acid

and two monoamines in rat plasma by HPLC–ECD/DAD. *J Pharm Biomed Anal.* 2018;158:8–14.

13. Von Dalowski F, Kramer M, Wermke M, et al. Mesenchymal Stromal Cells for Treatment of Acute Steroid–Refractory Graft Versus Host Disease: Clinical Responses and Long–Term Outcome. *Stem Cells.* 2016;34(2):357–366.
14. Filipovich AH, Weisdorf D, Pavletic S, et al. National Institutes of Health Consensus Development Project on Criteria for Clinical Trials in Chronic Graft–versus–Host Disease: I. Diagnosis and Staging Working Group Report. *Biol Blood Marrow Transplant.* 2005;11(12):945–956.
15. Chang C–L, Leu S, Sung H–C, et al. Impact of apoptotic adipose–derived mesenchymal stem cells on attenuating organ damage and reducing mortality in Rat sepsis syndrome induced by cecal puncture and ligation. *J Transl Med.* 2012;10(1):244.

Table 1. Patients' characteristics

| Diagnosis | Age & gender | Donor types | GvHD Grade | GvHD organs | Pre-MSC therapy | Conditioning Regimen | MSC (x10 ⁶ /Kg) | Response |
|-----------|--------------|-------------|------------|------------------|-------------------------------------|---|---------------------------------------|----------|
| B-ALL | 47, M | MSD, PBSCT | III | Skin, Liver | Steroids, ECP, CsA | Etoposide phosphate; TBI | 2.01 | NR |
| PMF | 63, M | MUD, PBSCT | III | Gut | CsA, Prednisolone | Busulfan Fludarabine | 1.02 | NR |
| sAML | 58, M | MUD, PBSCT | IV | Gut | CsA, Prednisolone | Busilvex Fludarabine | 1.02 | NR |
| MDS-EB2 | 67, M | PBSCT | IV | Liver, Gut | Steroids, Ruxolitinib | Fludarabine; Busulfan | 2.28 | NR |
| ALK-ALCL | 45, M | MSD, PBSCT | IV | Skin, Gut | Prednisolone, Ruxolitinib, MSC, MMF | Busilvex; Cyclophosphamide; Fludarabine | 2.23 [†] & 2.18 [‡] | PR |
| rAML | 62, F | MRD, PBSCT | IV | Liver, Gut | CsA, Prednisolone | Busilvex; Fludarabine | 2.28 | PR |
| MM | 68, M | MUD, PBSCT | IV | Gut | CsA, Prednisolone | Rhenium-anti-CD66; Fludarabine; Treosulfane | 1.05 | PR |
| AML | 58, M | PBSCT | IV | Skin, Liver, Gut | CsA, Prednisolone, ECP, Ruxolitinib | Fludarabine; Busulfan | 1.05 | PR |

†: First dose

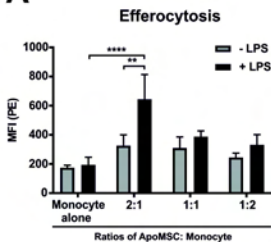
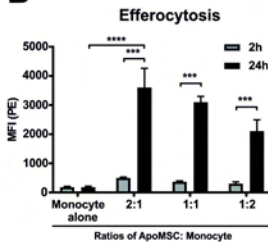
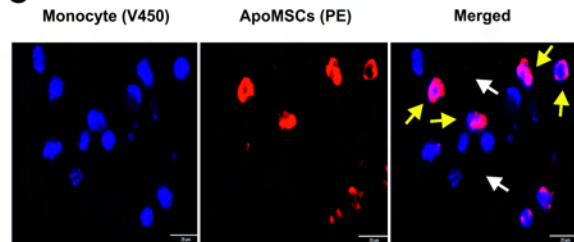
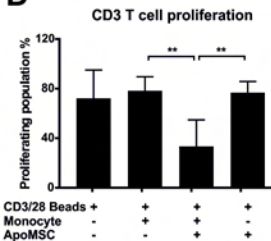
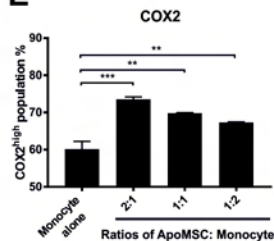
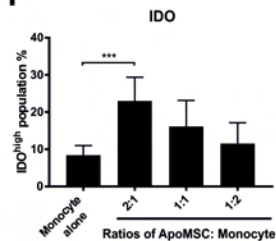
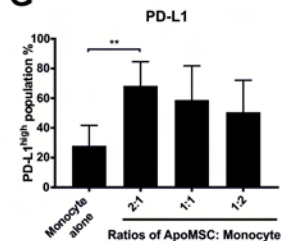
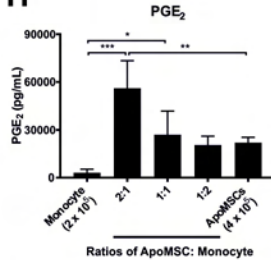
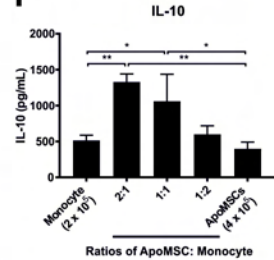
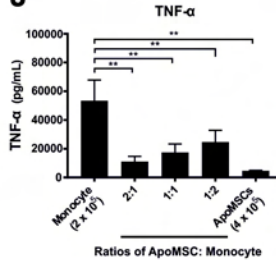
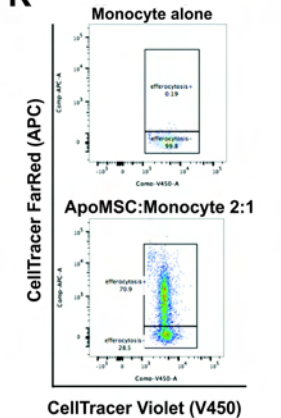
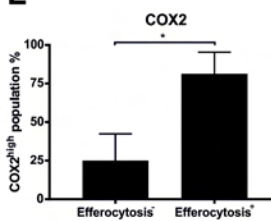
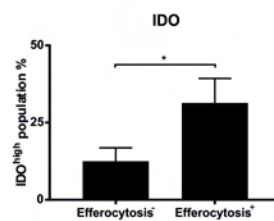
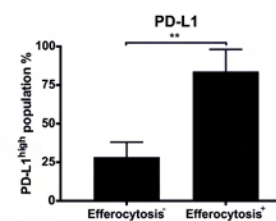
‡: Second dose

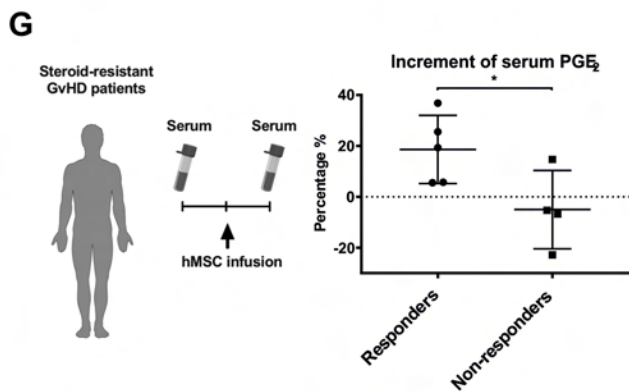
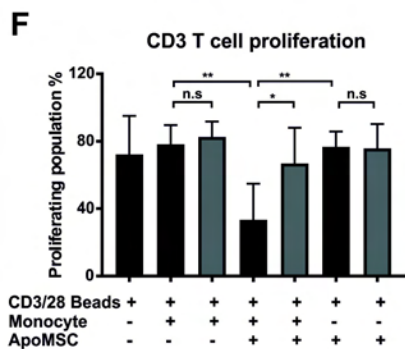
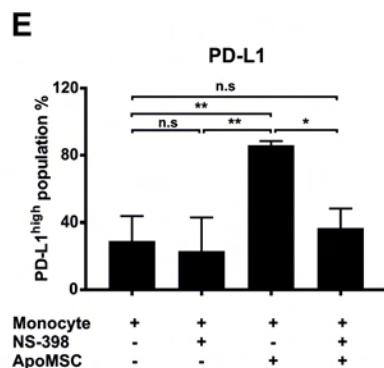
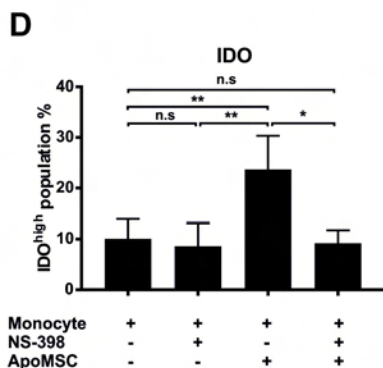
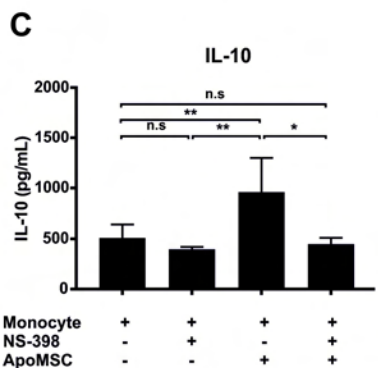
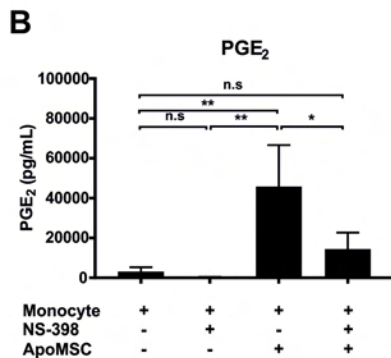
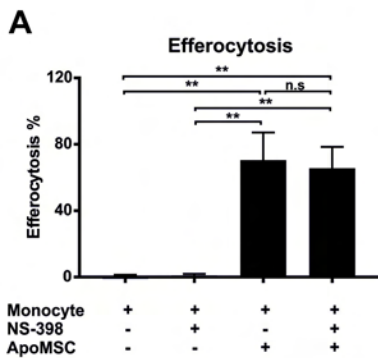
ALK-ALCL: Anaplastic Lymphoma Kinase-Negative Anaplastic Large Cell Lymphoma; AML: Acute Myeloid Leukemia; B-ALL: B-cell Acute Lymphoblastic Leukemia; CSA: Cyclosporine; ECP: Extracorporeal photopheresis; F: Female; M: Male; MDS-EB2: Myelodysplastic Syndrome with Excess Blasts Type 2; MM: Multiple Myeloma; MMF: Mycophenolate Mofetil; MRD: HLA-matched related donor; MSC: Mesenchymal stromal cells; MSD: HLA-matched sibling donor; MUD: HLA-matched unrelated donor; NR: non-responders; PBSCT: Peripheral Blood Stem Cell Transplant; PMF: Primary myelofibrosis; R: responders; rAML: Relapsed AML; sAML: Secondary AML; TBI: Total body irradiation

Figure legends

Figure 1. Efferocytosis of ApoMSCs polarizes monocytes into an immunosuppressive phenotype. (A) ApoMSCs were stained with 20 ng/mL pHrodo™ Red-succinimidyl ester (PE) whilst isolated monocytes were stained with 1 μ M CellTrace™Violet (V450). Monocytes were cultured with different amounts of ApoMSCs for 2 hours at 37°C, 5% CO₂. 100 μ g/mL LPS was used to stimulate monocytes. The MFI (PE) within the monocytes population was measured as an indicator of efferocytosis, n=3. (B) MFI (PE) after 2 and 24 hours was compared among the different groups, n=3. (C) Confocal images of monocytes efferocytosing ApoMSCs after 24 hours in culture. The yellow arrows indicate the monocytes engulfing ApoMSCs whilst the white arrows indicate ApoMSCs alone. Bar represents 20 μ m. (D) monocytes (2 x 10⁵/well) were co-cultured with ApoMSCs (4 x 10⁵/well) for 8 hours. CellTrace™ Violet-labelled CD3 T cells (2 x 10⁵/well) were added to the cultures and stimulated by CD3/CD28 beads at a 1:1 cell:bead ratio for 3 days. The percentage of proliferating T cells were measured by flow cytometry according to the loss of fluorescence intensity due to cell division, n=4. (E-G) Intracellular and surface stainings were performed to examine different kinds of protein expressions including COX2, IDO and PD-L1 in monocytes. The COX2^{high}, n=3 (E), IDO^{high}, n=4 (F) and PD-L1^{high}, n=3 (G) populations were gated according to the monocyte alone control (used as negative control). (H-J) ELISA was performed to assess the amount of PGE₂, n=4 (H), IL-10, n=3 (I) and TNF- α , n=6 (J) in cell culture supernatants. (K) To select the monocytes according to the efferocytosis, ApoMSCs were fluorescent-labelled with CellTrace™FarRed (APC⁺) whilst monocytes were labelled with CellTrace™Violet (V450⁺). APC⁺ Monocytes were regarded as efferocytosis⁺ and APC⁻ monocytes were regarded as efferocytosis⁻. (L) Bar charts showing the difference of COX2^{high}, IDO^{high} and PD-L1^{high} population between the efferocytosis⁺ and efferocytosis⁻ monocytes, n=3. Experimental data were expressed as mean \pm SD. Unpaired *t* test was used to compare the mean differences between two samples. One-way ANOVA and post-hoc Tukey test were used to compare the mean differences among the samples (* *p*-values < 0.05; ** *p*-values < 0.01; *** *p*-values < 0.001; **** *p*-values < 0.0001).

Figure 2. Efferocytosis-induced COX2/PGE₂ is the key effector molecule of immunosuppressive monocytes. (A) 100 μM NS-398 was added during the co-culture of monocytes and ApoMSCs. After 8-hours, efferocytosis was evaluated using flow cytometry, n=3. As reported in A, PGE₂, n=4 (B) and IL-10, n=4 (C) were evaluated in cell culture supernatant using ELISA, whilst IDO, n=5 (D) and PD-L1, n=3 (E) in monocytes were examined by flow-cytometry. (F) COX2 activity in efferocytosing monocytes was inhibited by using 100 μM NS-398 before adding them to CellTrace™ Violet-labelled CD3 T cells. Proliferation of T cells were measured and analyzed by flow cytometry, n=4. Experimental data were expressed as mean ± SD. One-way ANOVA and post-hoc Tukey test were used to compare the mean differences among the samples. (G) 8 steroid-resistant GvHD patients receiving MSC were analyzed for serum PGE₂ levels. The percentages of PGE₂ increment [$\text{PGE}_2^{\text{after infusion}} - \text{PGE}_2^{\text{before infusion}} / \text{PGE}_2^{\text{before infusion}} \times 100\%$] were compared between clinical responders (● n=5) and non-responders (■ n=4). Unpaired *t* test was used to compare the mean differences between two groups (* *p*-values < 0.05; ** *p*-values < 0.01; ns, not significant).

A**B****C****D****E****F****G****H****I****J****K****L****I****J**



Supplementary Materials to:

**Apoptotic mesenchymal stromal cells induce prostaglandin E₂ in monocytes:
implications for the monitoring of mesenchymal stromal cell activity**

Tik Shing Cheung¹, Antonio Galleu¹, Malte von Bonin², Martin Bornhäuser²,
Francesco Dazzi¹

¹School of Cancer and Pharmacological Sciences and KHP Cancer Research UK
Centre, King's College London, London, United Kingdom. ²University Hospital
Carl Gustav Carus, Dresden, Germany.

Corresponding author:

Francesco Dazzi

School of Cancer and Pharmacological Sciences and KHP Cancer Research UK
Centre

The Rayne Institute

King's College London

123, Coldharbour Lane

London SE5 9NU

francesco.dazzi@kcl.ac.uk

Supplementary Methods

MSC isolation and culture

Human bone marrow-derived MSCs were isolated from the bone marrow aspirate taken from the iliac crest of healthy donor, which was obtained from the Imperial College Healthcare Tissue Bank (ICHTB, HTA license 12275). ICHTB is supported by the National Institute for Health Research (NIHR) Biomedical Research Centre based at Imperial College Healthcare NHS Trust and Imperial College London. ICHTB is approved by the UK National Research Ethics Service to release human material for research (12/WA/0196), and the samples for this project were issued from the sub-collection. Informed consent was obtained in accordance with ICHTB requirements and procedures were carried out in accordance with relevant guidelines and regulations. Mononuclear cells were first plated ($10 - 25 \times 10^6$ per 636 cm^2) in MEM- α (Thermo Fisher Scientific) containing 5% (v/v) human platelet lysate (Cook Regentec) and 1 U/mL heparin (Wockhardt) at 37°C , 5% CO_2 . Non-adherent cells were removed after washing of PBS (Thermo Fisher Scientific) and replenishing the culture medium. When adherent MSCs reached approximately 70% to 90% confluence of culture flask, they were detached using Trypsin-EDTA (0.05%) with phenol red (Thermo Fisher Scientific) and expanded. MSCs at passage 3 to 7 (all from the same MSC donor) were used for experiments.

Generation of ApoMSCs

5×10^5 MSCs were treated with $10 \mu\text{g/mL}$ anti-Fas stimulating monoclonal antibody (CH11, Merck) in complete RPMI-1640 for 24 hours at 37°C , 5% CO_2 . Caspase activation was confirmed using pan-caspase inhibitor Z-VAD-FMK ($50 \mu\text{M}$, R&D Systems) under PE-Annexin V and 7-AAD (BD) staining using flow cytometry and caspase-3 (active) immunoblotting.

Protein extraction and Immunoblotting

Cell lysates from MSCs and ApoMSCs were homogenized using $100 \mu\text{L}$ radioimmunoprecipitation assay buffer with phenylmethanesulfonyl fluoride and protease inhibitors (all Thermo Fisher Scientific). After several vortexing and incubation on ice for 30 minutes, the protein extracts were obtained after centrifuging at $10,000 \text{ xg}$ for 15 mins at 4°C . The amount of protein was determined by bicinchoninic acid protein assay kit (Thermo Fisher Scientific).

Protein standards were prepared using bovine serum albumin (BSA) (Sigma–Aldrich) and deionized water. Amount of protein in samples was measured by NanoDrop™ 1000 Spectrophotometer (Thermo Fisher Scientific). Deionized water was used as blank. 20 µg protein per sample was prepared in Laemmli buffer (Thermo Fisher Scientific) and boiled at 100°C for 5 mins. Then, samples with equal protein amount were electrophoresed on 5–10% SDS–polyacrylamide gels and then transferred onto activated nitrocellulose membranes. After electroblotting, the membrane was washed by Tris–buffered saline–Tween20 (TBS–T) and 5 % (w/v) non–fat milk in TBS–T was used to block the membrane for 1 hour at room temperature. Discarding the blocking buffer, primary anti–caspase–3 (dilution 1:500, Cell Signaling Technology) in 3% BSA (w/v) TBS–T was added for overnight probing at 4°C. Anti–α–tubulin antibody (dilution 1:500, Santa Cruz Biotechnology) was used as protein loading control. Secondary antibody conjugated with horseradish peroxidase in 5% non–fat milk TBS–T (dilution 1:1000) was added for 1–hour incubation at room temperature followed by TBS–T washing. Protein expression was detected using Pierce™ ECL Western Blotting Substrate (Thermo Fisher Scientific). Membrane was imaged using Azure c300 Chemiluminescent Western Blot Imaging System.

Isolation of human PBMCs, monocytes and CD3 T cells

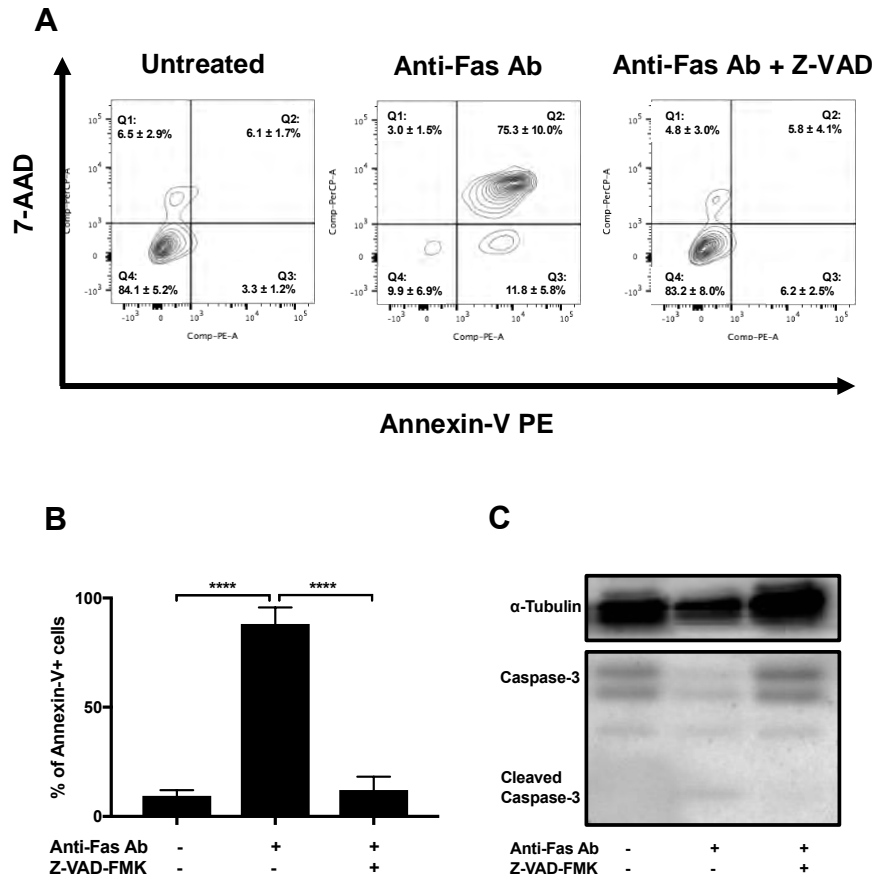
Human blood samples are purchased from the National Health Service (NHS) Blood and Transplant (UK) with the non–clinical account number (P243) for research purposes. For this project being conducted in England, no ethical approval is needed from the NHS Research Ethics Committee. Human peripheral blood mononuclear cells (PBMCs) were isolated from healthy volunteers' blood using Ficoll–Paque™ (Sigma–Aldrich). The storage of isolated human PBMCs is under the Human Tissue Authority (UK) license no.11023. To obtain monocytes and CD3 T cells, PBMCs were subjected to Pan Monocyte Isolation Kit II and CD3 MicroBeads (Miltenyi), respectively. After purification, CD14⁺ (61D3) cells were 91.9 ± 0.7 % (n=4), whilst CD3⁺ (UCHT1) cells were 96.7 ± 0.6% (n=3) compared to the isotype controls.

Statistical analysis

Statistical analysis was performed using PRISM version 6.0 (GraphPad, USA). Experimental data were expressed as mean ± SD from at least three

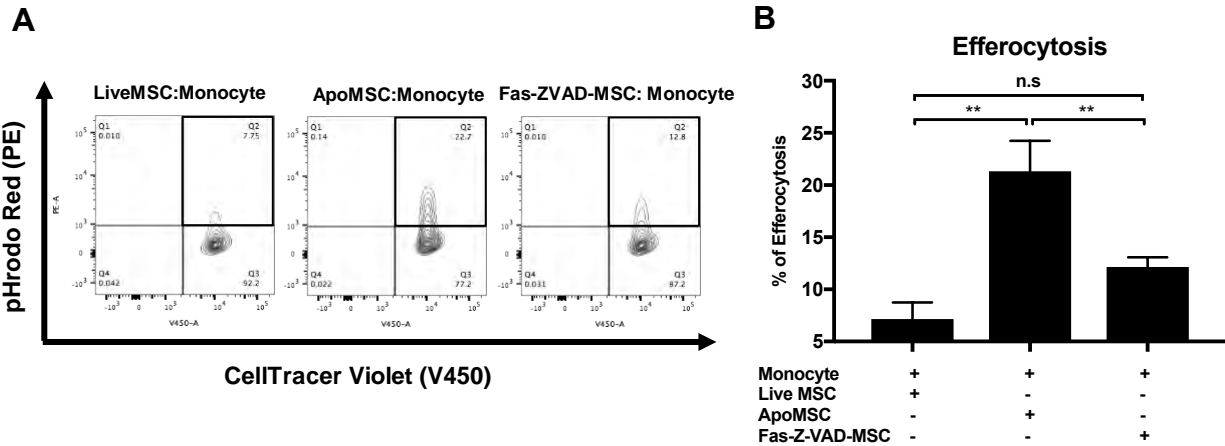
determinations. One-way ANOVA and post-hoc Tukey test were used to compare the mean differences when there are more than two samples. Unpaired t test was used to compare the mean differences between two samples. p values less than 0.05 were considered statistically significant.

Supplementary Figures



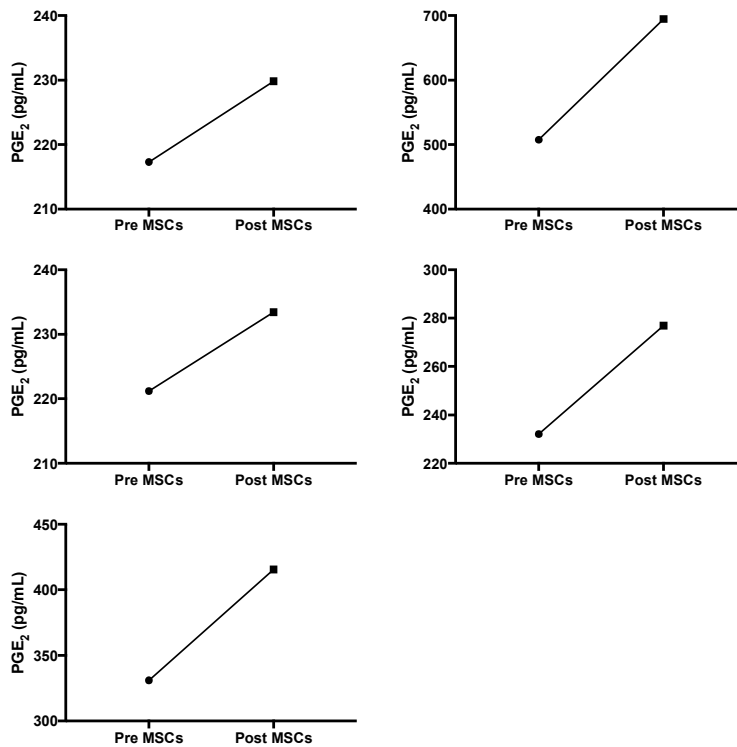
Supplementary Figure 1. Human bone marrow MSCs undergo Fas-stimulated apoptosis via caspase activation. (A) 5×10^5 MSCs were treated with $10 \mu\text{g}/\text{mL}$ anti-Fas stimulating monoclonal antibody (CH11) for 24 hours to induce apoptosis. Apoptosis was assessed using the PE-annexin-V and 7-AAD by flow cytometry. Gating strategy and representative plots annotated with experiment data (mean \pm SD in each quadrant) are shown, $n=5$. Pan-caspase inhibitor Z-VAD-FMK ($50\mu\text{M}$) was added during the incubation to examine the dependence of caspase activation following the Fas-stimulation (B). The percentage of apoptotic cells was calculated as Annexin-V⁺ cells by adding the percentage of cell population in the Q2 upper-right quadrant (Annexin-v⁺ and 7-AAD⁺) and Q2 lower-right quadrant (Annexin-v⁺ and 7-AAD⁻). Experimental data were expressed as mean \pm SD, $n=5$. One-way ANOVA and post-hoc Tukey test were used to compare the mean differences among the samples (**** p -values <

0.0001). (C) The protein lysates were extracted and performed immunoblotting with anti-caspase-3 (dilution 1:500) and anti- α -tubulin antibody (dilution 1:500). Dilution of secondary antibody conjugated with horseradish peroxidase was 1:1000. The image is the representative from 3 experiments.

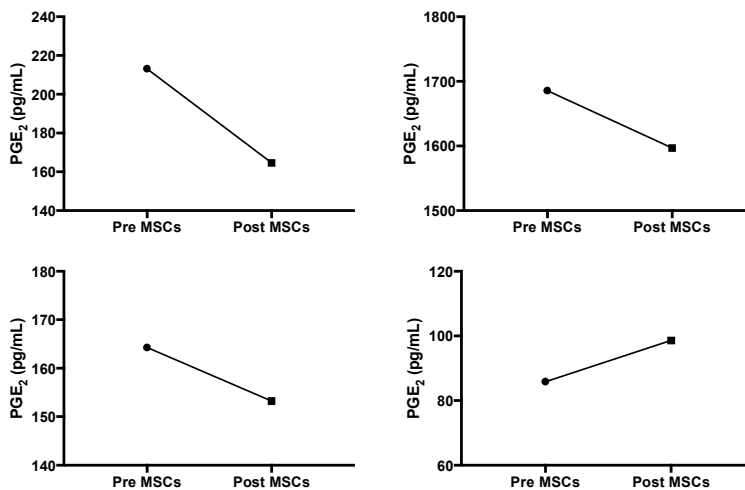


Supplementary Figure 2. Efferocytosis is selective for ApoMSCs. (A) LPS-activated monocytes were co-cultured with non-apoptotic MSCs (Live MSCs, untreated; Fas-ZVAD-MSC, MSCs treated with anti-Fas and caspase inhibitor Z-VAD-FMK) or ApoMSCs under the same co-culture ratio (MSCs: Monocytes 2:1) for 2 hours before efferocytosis was assessed. All groups of MSCs were fluorescent-labelled with 20 ng/mL pH-sensitive fluorescent dye pHrodo™Red. Monocytes undergoing efferocytosis were considered as V450⁺ population acquiring the PE fluorescence (Q2 upper-right quadrant: V450⁺ and PE⁺). (B) Percentage of efferocytosis was determined according to the population of Q2 quadrant. Experimental data were expressed as mean \pm SD, n=4. One-way ANOVA and post-hoc Tukey test were used to compare the mean differences among the samples (** *p*-values < 0.01; ns, not significant).

A Changes of serum PGE₂ in PR



B Changes of serum PGE₂ in NR



Supplementary Figure 3. Change of serum PGE₂ level in responder (A) and non-responder (B) GvHD patients. For each patient, the sera before MSC treatment

(Pre MSCs) and after MSC treatment (Post MSCs) have been examined for the level of PGE₂ using ELISA kit.